Elliptic flow and system size dependence of transition energies at intermediate energies

Yingxun Zhang[1,*] and Zhuxia Li[1,2,3,†]
[1]*China Institute of Atomic Energy, P.O. Box 275 (18), Beijing 102413, People's Republic of China*
[2]*Center of Theoretical Nuclear Physics, National Laboratory of Lanzhou Heavy Ion Accelerator, Lanzhou 730000, People's Republic of China*
[3]*Institute of Theoretical Physics, Chinese Academic of Science, Beijing 100080, People's Republic of China*
(Received 12 December 2005; published 7 July 2006)

The elliptic flow for $Z \leqslant 2$ particles in heavy ion collisions at energies from several tens to several hundreds MeV per nucleon is investigated by means of a transport model, i.e., a new version of the improved quantum molecular dynamics model (ImQMD05). This model employs a complete Skyrme potential energy density functional. The influence of different effective interactions and medium corrections of nucleon-nucleon cross sections on the elliptic flow are studied. Our results show that a soft nuclear equation of state and incident energy dependent in-medium nucleon-nucleon cross sections are required to describe the excitation function of the elliptic flow at intermediate energies. The size dependence of transition energies for the elliptic flow at intermediate energies is also studied. The system size dependence of transition energies fits a power of system size with an exponent of 0.223.

DOI: 10.1103/PhysRevC.74.014602 PACS number(s): 25.70.−z, 24.10.Lx, 21.65.+f

A main goal of the research area of heavy ion collisions (HICs) at intermediate energies is to extract more accurate information on the nuclear equation of state (EoS). Considerable progress has been made recently in determining the equation of state of nuclear matter from heavy ion reaction data [1–5]. A prominent role among available observables is played by collective flow. Much theoretical and experimental effort has been expended on the study of collective flow in HICs [6–23]. The elliptic flow has proven to be one of the more fruitful probes for extracting the EoS and the dynamics of heavy ion collisions. The parameter of elliptic flow is quantified by the second-order Fourier coefficient $v_2 = \langle \cos 2\phi \rangle = \langle \frac{p_x^2 - p_y^2}{p_x^2 + p_y^2} \rangle$ from the azimuthal distribution of detected particles at midrapidity as

$$\frac{dN}{d\phi} = P_0(1 + 2v_1 \cos\phi + 2v_2 \cos 2\phi), \tag{1}$$

where ϕ is the azimuthal angle of the emitted particle momentum relative to the x axis. Positive values for $\langle \cos 2\phi \rangle$ reflect a preferential in-plane emission, and negative values for $\langle \cos 2\phi \rangle$ reflect a preferential out-of-plane emission. The change of sign recently observed at ultrarelativistic energies has received particular interest as it reflects the increasing pressure buildup in the nonisotropic collision zone [24]. Recently, the excitation function of elliptic flow parameters at energies from Fermi energy to the relativistic energy regime for ^{197}Au+^{197}Au has been measured by the FOPI, INDRA, and ALADIN Collaborations [6,7], and the transition energy from positive to negative elliptic flow was confirmed, which is around 100 MeV/nucleon. The elliptical flow parameters $\langle \cos 2\phi \rangle$ at energies from tens to hundreds of MeV per nucleon are determined by the complex interplay among expansion, rotation, and the shadowing of spectators. Both the mean field and two-body collision parts play important roles in this energy region. The mean field plays a dominant role at low energies, and then gradually the two-body collision becomes dominant with energy increases. Thus, a detailed study of the excitation function of elliptical flow in this energy region can provide more useful information on the nucleon-nucleon interaction related to the equation of state of nuclear matter and the medium correction of nucleon-nucleon cross sections. The transition energy of elliptic flow at intermediate energies may be particularly useful in extracting information on the nuclear effective interaction. While elliptic flow at energies higher than the transition energy will be useful in extracting the medium correction of nucleon-nucleon cross sections because two-body collisions play a more important role on collective flow at these energies [9,23,25]. Another aim of this work is to investigate the medium correction of nucleon-nucleon cross sections through elliptic flow in heavy ion collisions at energies from the Fermi energy to relativistic energies.

In this report, we apply the new version of the improved quantum molecular dynamics model (ImQMD05) to study the excitation function of elliptic flow parameters for ^{197}Au+^{197}Au at intermediate energies, and through the comparison between measurement and model calculations to extract the information on the effective interaction related to the EoS and the medium correction of nucleon-nucleon cross sections. The system size dependence of transition energies of elliptic flow from ^{58}Ni+^{58}Ni to ^{197}Au+^{197}Au will also be studied.

For the convenience of the readers, we first give a brief introduction of the ImQMD05 model. The main developments of the ImQMD model compared with the usual IQMD model are the introduction of (1) the isospin independent and dependent surface energy terms in the energy density functional, (2) the constraint on the single-particle occupation number, and (3) the system size dependent wave packet width [26]. The ImQMD model can successfully describe the yields of clusters in intermediate energy heavy ion collisions [27]. In the ImQMD05 model, we introduce the full Skyrme potential energy density functional except for the spin-orbit term in

*Electronic address: zhyx@iris.ciae.ac.cn
†Electronic address: lizwux@iris.ciae.ac.cn

the local interaction part, which allows us to choose various Skyrme interactions that describe the ground states of nuclei and saturated nuclear matter similarly well but predict rather different properties away from saturated density.

In the ImQMD05 model, the nuclear local interaction potential energy density functional $V_{\rm loc}(\rho(\mathbf{r}))$ reads

$$\begin{aligned} V_{\rm loc} &= \frac{\alpha}{2}\frac{\rho^2}{\rho_0} + \frac{\beta}{\gamma+1}\frac{\rho^{\gamma+1}}{\rho_0^{\gamma}} + \frac{g_{\rm sur}}{2\rho_0}(\nabla\rho)^2 \\ &\quad + \frac{g_{\rm sur,iso}}{\rho_0}[\nabla(\rho_n-\rho_p)]^2 + (A\rho^2 + B\rho^{\gamma+1} + C\rho^{8/3})\delta^2 \\ &\quad + g_{\rho\tau}\frac{\rho^{8/3}}{\rho_0^{5/3}}, \end{aligned} \tag{2}$$

where ρ, ρ_n, ρ_p are the nucleon, neutron, and proton density, and $\delta = (\rho_n-\rho_p)/(\rho_n+\rho_p)$ is the isospin asymmetry. The first two terms in expression (2) are the isoscalar bulk energy part, the third term is the isospin independent surface energy term, the fourth term is the surface symmetry energy term, and the fifth term is the bulk symmetry energy term. The last term, called the $\rho\tau$ term, is obtained from the $\rho\tau$ term of the Skyrme potential energy density functional by applying the Thomas-Fermi approximation to the kinetic energy density τ, and thus the explicit momentum dependence is lost. However, the strength of this term $g_{\rho\tau}$ is rather small compared with other isoscalar terms. The coefficients in expression (2) are therefore directly related to the standard Skyrme interaction parameters as

$$\begin{aligned} \frac{\alpha}{2} &= \frac{3}{8}t_0\rho_0, \qquad \frac{\beta}{\gamma+1} = \frac{1}{16}t_3\rho_0^{\gamma}, \\ \frac{g_{\rm sur}}{2} &= \frac{1}{64}(9t_1 - 5t_2 - 4x_2t_2)\rho_0, \\ \frac{g_{\rm sur,iso}}{2} &= -\frac{1}{64}(3t_1(2x_1+1) + t_2(2x_2+1))\rho_0. \end{aligned} \tag{3}$$

A, B, and C in the volume symmetry energy term are also given by the Skyrme interaction parameters as

$$\begin{aligned} A &= -\frac{t_0}{4}(x_0+1/2), \\ B &= -\frac{t_3}{4}(x_3+1/2), \\ C &= -\frac{1}{24}\left(\frac{3\pi^2}{2}\right)^{2/3}\Theta_{\rm sym}, \end{aligned} \tag{4}$$

where $\Theta_{\rm sym} = 3t_1x_1 - t_2(4+5x_2)$. $g_{\rho\tau}$ is determined by

$$g_{\rho\tau} = \frac{3}{80}(3t_1 + (5+4x_2)t_2)\left(\frac{3\pi}{2}\right)^{2/3}\rho_0^{5/3}. \tag{5}$$

The t_0, t_1, t_2, t_3 and x_0, x_1, x_2, x_3 in expressions (3)–(5) are the parameters of Skyrme force. In the calculations performed in this work, for the bulk symmetry potential energy density, we only take the ρ^2 form, which corresponds to the form of the linear density dependence of the symmetry potential energy that people usually use, but the symmetry energy coefficient is calculated with the full energy density functional given by (2). The symmetry potential energy should not play an important role in the quantity studied in this work. Furthermore, we introduce an explicit momentum dependent term in the same form as that in [28], which reads

$$U_{\rm MD} = 1.57[\ln(1 + 5\times 10^{-4}\Delta p^2)]^2\rho/\rho_0, \tag{6}$$

as we find the explicit momentum dependent term is important for elliptic flow. This term provides an effective mass $m^*/m = (1 + m/p dU_{\rm MD}/dp)$, which is about 0.75 at the Fermi momentum and about 0.95 at a relative momentum around 800 MeV/nucleon [28]. The calculations show that without an explicit momentum dependent term, the behavior of the calculated excitation function of elliptic flow is not consistent with that of experiments, no matter which interaction is adopted. This finding agrees with the conclusion obtained in [16]. The Coulomb interaction potential energy is also introduced. By using the present model, we can directly test effective interactions, specifically, the various Skyrme interactions characterized by different K and m^*/m of EoS, by comparing the predictions of different Skyrme interactions with measurement of elliptic flow. In this work, SkP [29], SkM* [30], SLy7 [31], and SIII [32] interactions are chosen. The first three are with similar incompressibility $K_\infty \sim 200$–229 MeV but with different m^*/m; the last one is with $K_\infty \sim 354$ MeV. Table I gives the parameters in the energy density functional (2) and the properties of saturated nuclear matter for the Skyrme interactions employed in this work.

The collision term, in which the phenomenological density dependent in-medium nucleon-nucleon cross sections are taken, reads

$$\sigma_{nn}^* = (1 - \eta\rho/\rho_0)\sigma_{nn}^{\rm free}, \tag{7}$$

where $\sigma_{nn}^{\rm free}$ denotes the free nucleon-nucleon scattering cross sections [33], which are isospin dependent. In the treatment of Pauli blocking in the collision part, neutrons and protons are treated separately, and two criteria are used as in [34],

$$\frac{4\pi}{3}r_{ij}^3\frac{4\pi}{3}p_{ij}^3 \geqslant \frac{h^3}{8} \tag{8}$$

and

$$P_{\rm block} = 1 - (1-f_i)(1-f_j), \tag{9}$$

TABLE I. ImQMD model parameters and properties of saturated nuclear matter for Skryme interactions employed in this work.

	SkP	SkM*	SLy7	SIII
α(MeV)	−356.20	−317.40	−293.97	−122.75
β(MeV)	303.03	248.96	215.03	55.19
γ	7/6	7/6	7/6	2
$g_{\rm sur}$(MeV fm^2)	19.47	21.82	22.64	18.26
$g_{\rm sur,iso}$(MeV fm^2)	−11.35	−5.47	−2.25	−4.94
$g_{\rho\tau}$(MeV)	0.00	5.92	9.92	6.42
m^*/m	1.00	0.789	0.687	0.763
ρ_∞(fm^{-3})	0.162	0.160	0.158	0.145
a_s(MeV)	30.66	30.68	32.62	28.78
K_∞(MeV)	200	216	229	354

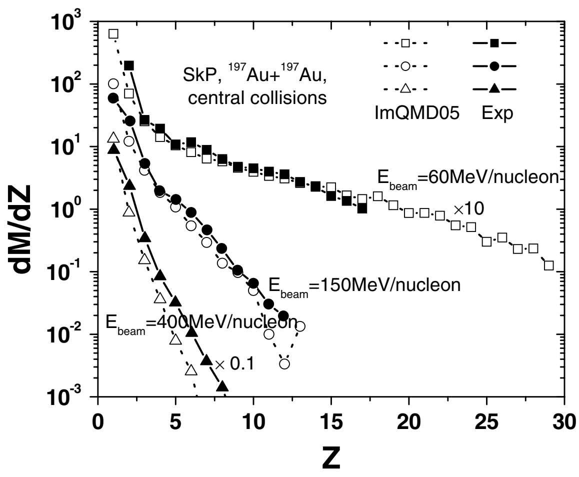

FIG. 1. Charge distributions of products in the central collisions of reactions ^{197}Au+^{197}Au at $E_{\rm beam} = 60$, 150, 400 MeV/nucleon calculated with the ImQMD05 model. The SkP Skyrme interaction is chosen. Experimental data (solid symbols) are taken from [35,36]. Calculation results are for products at the same forward angles as those used for the experimental data.

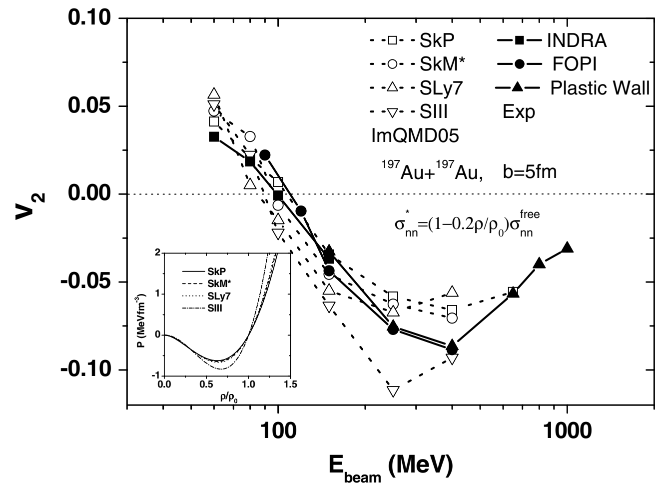

FIG. 2. Excitation functions of elliptic flow parameters at midrapidity for $Z \leqslant 2$ particles from midcentral collisions of ^{197}Au+^{197}Au calculated with SkP, SkM*, SLy7, and SIII Skyrme interactions. The calculated results are given in the same rotated reference frame as that used for the experimental data, which are taken from [6]. Inset shows pressure as a function of density calculated with the four Skyrme interactions.

where f_i is the phase space distribution function for nucleon i.

The fragments are constructed by means of the coalescence model widely used in the QMD model calculations in which particles with relative momenta smaller than P_0 and relative distances smaller than R_0 are coalesced into one cluster (here, $R_0 = 3.0$ fm and $P_0 = 250$ MeV/c are adopted). Figure 1 shows the charge distribution of fragments for ^{197}Au+^{197}Au at $E_{\rm beam} = 60, 150, 400$ MeV/nucleon at central collisions, respectively. One sees from the figure that the calculation results for charge distribution of fragments are in good agreement with experimental data. Then, we apply the ImQMD05 model to study the excitation function of elliptic flow parameters and try to extract the information on the effective interactions and the medium corrections of two-body cross sections.

Figure 2 shows the excitation function of elliptic flow parameters at midrapidity ($|y/y_{\rm mc}^{\rm proj}| \leqslant 0.1$) for $Z \leqslant 2$ particles for ^{197}Au+^{197}Au collisions at $b = 5$ fm [the reduced impact parameter $b/b_{\rm max}$ equals 0.38 and $b_{\rm max} = 1.15(A_P^{1/3}+A_T^{1/3})$]. The calculated elliptic flow is given in the same rotated reference frame as that for the experimental data. In the figure, solid symbols denote experimental data [3,6,7] and open symbols denote calculation results with Skyrme interactions SkP, SkM∗, SLy7, and SIII. Concerning the in-medium two-body cross sections, the η in expression (6) is taken to be 0.2. The general behavior of the excitation functions of elliptical flow parameters v_2 calculated with different Skyrme interactions are similar, i.e., the elliptic flow evolves from a preferential in-plane (rotational like) emission ($v_2 > 0$) to out-of-plane (squeeze out) emission ($v_2 < 0$) with an increase of energies. But the detailed behavior of the results from different Skyrme interactions are rather different. One can see from the figure that the transition energies at which the elliptic flow parameter (v_2) changes sign from positive to negative are divergent for different Skyrme interactions. The difference is more than 30 MeV/nucleon among the calculation results with Skyrme interactions SkP, SkM*, SLy7, and SIII. The transition from preferential in-plane emission to out-of-plane emission occurs because the mean field which contributes to the formation of a rotating compound system becomes less important and the collective expansion process based on the nucleon-nucleon scattering starts to be predominant. The competition between the mean field and the nucleon-nucleon collisions should strongly depend on the effective interaction, which leads to the divergence of the transition energies calculated with different Skyrme interactions. Clearly, the harder EoS provides stronger pressure which leads to a stronger out-of plane emission and thus to a smaller transition energy. The transition energies calculated with SkP and SkM* agree with experimental data, while those with SIII and SLy7 are too small compared with experimental data. To see the relation between the elliptic flow and the EoS, in the inset in Fig. 2, we show the pressure as a function of density calculated from the potential energy density functional (2) for SkP, SkM*, SLy7, SIII interactions. One can see that the transition energy sensitively depends on the stiffness of the EoS, which depends on both K and m^*/m. Thus, the best fit to the transition energy of the elliptic flow at intermediate energies provides us with information on the stiffness of the EoS. It seems to us that one needs multiple observables in order to explicitly extract K and m^*/m (also see [7,16]).

As energy further increases, v_2 becomes negative, and it reaches maximal negative value around 400 MeV/nucleon for SkP and SkM* and 250 for SLy7 and SIII. The calculations with SIII and SLy7 provide stronger pressure at the compression zone compared with SkP and SkM*, which makes calculated elliptic flow to reach the maximal negative v_2 at lower energy for SIII and SLy7. In comparing the predictions made with the four Skyrme interactions with

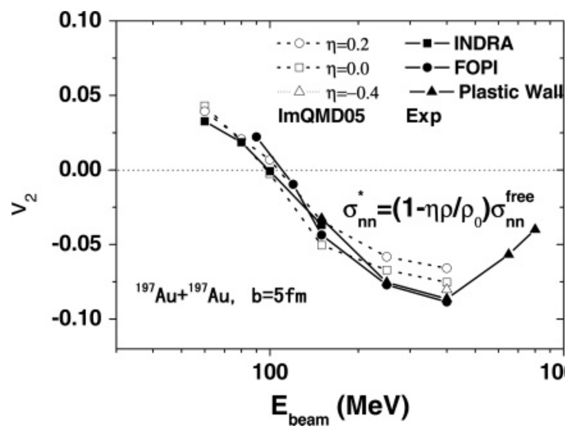

FIG. 3. Excitation functions of elliptic flow parameters at midrapidity for $Z \leqslant 2$ particles from midcentral collisions of ^{197}Au+^{197}Au with $\eta = 0.2$, 0.0, and -0.4 in the phenomenological expression of in-medium cross sections (6). SkP interaction is chosen. Experimental data are taken from [6].

measurements, we find that the results with SkP and SkM* are in reasonable agreement with experimental data. After reaching the maximal negative elliptic flow, the negative v_2 value decreases again. This implies that the spectator moves faster after the v_2 reaches the maximal negative value [7]. In Ref. [37], the nuclear stopping from 90 MeV/nucleon to 1.93 GeV/nucleon was measured and maximal nuclear stopping was observed around 400 MeV/nucleon for ^{197}Au+^{197}Au. It seems to us that the energy for reaching the maximal negative elliptic flow parameter is coincident with the energy for reaching the maximal nuclear stopping. It is clear that if the reaction system reaches the maximal stopping around certain energies, the matter formed in the reaction should reach minimal transparency, and thus most particles are preferentially emitted out of plane.

Now, let us investigate the influence of the medium correction of nucleon-nucleon cross sections on elliptic flow. Figure 3 shows the excitation functions of elliptic flow parameters calculated with $\eta = 0.2, 0.0, -0.4$ in expression (6), by which we effectively study the medium correction of nucleon-nucleon cross sections at different nuclear environments as well as the relative momentum of the scattering pair. The SkP Skyrme interaction is adopted in the calculations of Fig. 3. From the figure, we see that at energies lower than transition energy, the difference between the calculation results with $\eta = 0.2$ and $\eta = 0.0$ is small, both give reasonable agreement with experimental data, and the difference increases when the bombarding energy is higher than transition energy. As energy further increases, the negative elliptic flow calculated with $\eta = 0.2$ is too weak (i.e., too small of a negative elliptic flow parameter). One needs a smaller η or even a negative η. We find a reasonable agreement with experimental results can be obtained for the case at incident energy around 400 MeV/nucleon when η is taken to be about -0.4; i.e., at the energy of about 400 MeV/nucleon, the in-medium two-body cross section extracted is larger than the free cross section. In [38,39], it was predicted that the behavior of the in-medium elastic nucleon-nucleon cross section at supernormal densities as a function of the relative momentum of two colliding nuclei is first suppression and then enhancement. It is also predicted that the in-medium elastic nucleon-nucleon cross section increases with temperature. If we simply consider the relative momentum of a colliding nucleon pair to be roughly equal to the relative momentum of a projectile and target, and suppose the temperature increases obviously from several tens to several hundreds of MeV per nucleon, the information on the in-medium nucleon-nucleon cross sections extracted from the elliptic flow is qualitatively consistent with the prediction of [38,39]. This study suggests that the η in the phenomenological expression of in-medium nucleon-nucleon cross section (6) should depend on the reaction energy in order to mimic the medium correction of nucleon-nucleon cross sections at different environments. To confirm this finding, we make similar calculations for the excitation function of nuclear stopping in Au+Au at SIS energies and compared our results with measurements [37]. The information about the medium correction of the two-body cross section extracted from nuclear stopping is in good agreement with that obtained from the excitation function of elliptic flow in this work. The results concerning nuclear stopping will be given in another publication.

We notice that the calculation results are not in full agreement with measurements in the whole energy region. This means that a more self-consistent treatment including the in-medium cross section and the mean field and, especially, a more self-consistent explicitly momentum dependent term is needed, but this has been difficult to do.

We further carry out the study of the system size dependence for the elliptic flow of $Z \leqslant 2$ particles in ^{58}Ni+^{58}Ni, ^{112}Sn+^{112}Sn, and ^{197}Au+^{197}Au. We find that the transition energies for the three systems are obviously different. We then make a systematic investigation of the system size dependence of the transition energies of elliptic flow at an intermediate energy regime. Figure 4 shows the transition energies as a function of combined system mass. All reactions calculated are of symmetric reactions, the reduced impact parameters are chosen to be 0.38. The SkP Skryme interaction and $\eta = 0.2$ in the phenomenological expression

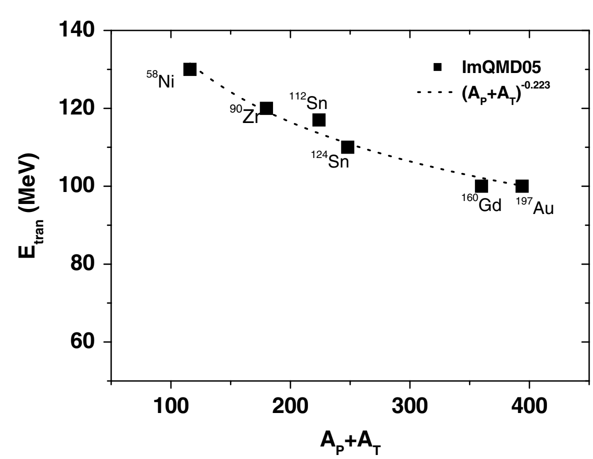

FIG. 4. Transition energies for elliptic flow at intermediate energies as a function of combined system mass.

(6) are adopted. From the figure, we see that the transition energy decreases as the reaction system size increases. One of the important reasons is that the pressure produced by the Coulomb interaction increases with the system size. We fit this curve with the following power law,

$$E_{\text{tran}} = x(A_P + A_T)^{-\tau}. \quad (10)$$

The exponent τ is about 0.223. Here, the exponent is substantially smaller than the exponent of the size dependence of balance energies for directed flow. Presumably, it is because more complex effects such as the expansion of the compressed zone and the shadowing effect of the colder spectator matter play roles in changing the sign of elliptic flow compared with the directed flow.

In summary, we have investigated the elliptic flow in heavy ion collisions at energies from several tens to several hundreds of MeV/nucleon with the ImQMD05 model. By changing the Skyrme interactions, we studied the influence of the EoS on elliptic flow, especially on the transition energy and the energy at which elliptic flow parameter reaches the maximal negative value. We find that the SkP and SkM* interactions can better describe the excitation function of elliptic flow at intermediate energies. The medium correction of nucleon-nucleon cross sections is also studied by changing the parameter η in expression (6). By fitting the experimental excitation function of elliptic flow parameters, we obtain the behavior of in-medium two-nucleon cross sections as a function of relative momentum of two colliding nucleons. Our study suggests that the medium correction (the η value) in the phenomenological expression of in-medium cross sections should depend on the relative momentum of the colliding pair and the medium density and temperature of the nuclear medium. The linear density dependence of the in-medium nucleon-nucleon cross section in (6) would probably be better validated when the incident energies are lower than 100 MeV/nucleon for HIC with heavy nuclear systems. The system size dependence of the transition energies was also investigated and found to fit a power of system size with an exponent of 0.223.

ACKNOWLEDGMENTS

We thank Dr. P. Danielewicz for helpful discussions. This work is supported by the National Natural Science Foundation of China under Grant Nos. 10175093, 10235030, and 10235020 and by the Major State Basic Research Development Program under Contract No. G20000774.

[1] P. Danielewicz, R. Lacey, and W. G. Lynch, Science **298**, 1592 (2002).
[2] M. Demoulins *et al.*, Phys. Lett. **B241**, 476 (1990).
[3] H. H. Gutbrod *et al.*, Phys. Lett. **B216**, 267 (1989); H. H. Gutbrod, K. H. Kampert, B. Kolb, A. M. Poskanzer, H. G. Ritter, R. Schicker, and H. R. Schmidt, Phys. Rev. C **42**, 640 (1990).
[4] W. Reisdorf and H. G. Ritter, Annu. Rev. Nucl. Sci. **47**, 663 (1997).
[5] H. Stöcker and W. Greiner, Phys. Rep. **137**, 277 (1986).
[6] J. Lukasik, G. Auger, M. L. Begemann-Blaich *et al.*, Phys. Lett. **B608**, 223 (2005).
[7] A. Andronic *et al.*, Nucl. Phys. **A679**, 765 (2001); Phys. Lett. **B612**, 173 (2005).
[8] W. Q. Shen *et al.*, Phys. Rev. C **57**, 1508 (1998).
[9] L. W. Chen and C. M. Ko, Phys. Lett. **B634**, 205 (2006); Phys. Rev. C **73**, 014906 (2006).
[10] M. B. Tsang *et al.*, Phys. Rev. C **53**, 1959 (1996).
[11] S. Wang *et al.*, Phys. Rev. Lett. **76**, 3911 (1996).
[12] C. Pinkenberg, N. N. Ajitanand *et al.*, Phys. Rev. Lett. **83**, 1295 (1993).
[13] Y. M. Zheng, C. M. Ko, B. A. Li, and B. Zhang, Phys. Rev. Lett. **83**, 2534 (1999).
[14] B. A. Li, A. T. Sustich, and B. Zhang, Phys. Rev. C **64**, 054604 (2001).
[15] A. B. Larionov, W. Cassing, C. Greiner, and U. Mosel, Phys. Rev. C **62**, 064611 (2000).
[16] P. Danielewicz, Nucl. Phys. **A673**, 375 (2000).
[17] D. Persram and C. Gale, Phys. Rev. C **65**, 064611 (2002).
[18] N. Bastid *et al.*, Nucl. Phys. **A622**, 573 (1997).
[19] C. Alt *et al.*, Phys. Rev. C **68**, 034903 (2003).
[20] K. H. Ackermann *et al.*, Phys. Rev. Lett. **86**, 402 (2001).
[21] G. D. Westfall, W. Bauer *et al.*, Phys. Rev. Lett. **71**, 1986 (1993).
[22] D. Klakow, G. Welke, and W. Bauer, Phys. Rev. C **48**, 1982 (1993).
[23] Hongbo Zhou, Zhuxia Li, and Yizhong Zhuo, Phys. Rev. C **50**, R2664 (1994); Nucl. Phys. **A580**, 627 (1994).
[24] C. Adler *et al.*, Phys. Rev. Lett. **90**, 032301 (2003); Phys. Rev. Lett. **91**, 182301 (2003).
[25] B. Zhang, L. W. Chen, and C. M. Ko, Phys. Rev. C **72**, 024906 (2005).
[26] Ning Wang, Zhuxia Li, and Xizhen Wu, Phys. Rev. C **65**, 064608 (2002); N. Wang, Z. Li, and X. Wu, Phys. Rev. C **69**, 034608 (2004).
[27] Yingxun Zhang and Zhuxia Li, Phys. Rev. C **71**, 024604 (2005).
[28] J. Aichelin, A. Rosenhauer, G. Peilert, H. Stoeker, and W. Greiner, Phys. Rev. Lett. **58**, 1926 (1987).
[29] J. Dobaczewski, H. Flocard, and J. Treiner, Nucl. Phys. **A422**, 103 (1997).
[30] J. Bartel, P. Quentin, C. Guet, and H.-B. Hakensson, Nucl. Phys. **A386**, 79 (1982).
[31] E. Chabanat, P. Bonche, P. H. Haensel *et al.*, Nucl. Phys. **A627**, 710 (1997).
[32] M. Beiner, H. Flocard, N. Van Giai, and P. Quentin, Nucl. Phys. **A238**, 29 (1975).
[33] J. Cugnon, D. L'Hôte, and J. Vandermeulen, Nucl. Instrum. Methods Phys. Res. B **111**, 215 (1996).
[34] Qingfeng Li and Zhuxia Li, Mod. Phys. Lett. A **17**, 375 (2002).
[35] W. Trautmann, A. Le Fèvre, and J. Lukasik (INDRA and ALADIN Collaborations), in *Proceedings of XLII International Winter Meeting on Nuclear Physics, Bormio, Italy, Jan 25–Feb 1, 2004*.
[36] W. Reisdorf, Prog. Theor. Phys. Supplement **140**, 111 (2000).
[37] W. Reisdorf *et al.* (FOPI Collaboration) Phys. Rev. Lett. **92**, 232301 (2004).
[38] Qingfeng Li, Zhuxia Li, and Guangjun Mao, Phys. Rev. C **62**, 014606 (2000).
[39] Qingfeng Li, Zhuxia Li, and Enguang Zhao, Phys. Rev. C **69**, 017601 (2004).